Electrogenerated Chemiluminescence for Chronopotentiometric Sensors

Gao, Wenyue; Jeanneret Grosjean, Stéphane; Yuan, Dajing; Cherubini, Thomas John; Wang, Lu; Xie, Xiaojiang; Bakker, Eric

How to cite

GAO, Wenyue et al. Electrogenerated Chemiluminescence for Chronopotentiometric Sensors. In: Analytical Chemistry, 2019, vol. 91, n° 7, p. 4889–4895. doi: 10.1021/acs.analchem.9b00787

This publication URL: https://archive-ouverte.unige.ch/unige:122441

Publication DOI: 10.1021/acs.analchem.9b00787

Electrogenerated Chemiluminescence for Chronopotentiometric Sensors

Wenyue Gao,[†,‡] Stéphane Jeanneret,[†] Dajing Yuan,[†] Thomas Cherubini,[†] Lu Wang,[†] Xiaojiang Xie[‡,*] and Eric Bakker[†,*]

[†] Department of Inorganic and Analytical Chemistry, University of Geneva, Quai Ernest-Ansermet 30, CH-1211 Geneva, Switzerland

[‡] Department of Chemistry, Southern University of Science and Technology, Shenzhen, 518055, China

ABSTRACT: We introduce here a general strategy to read out chronopotentiometric sensors by electrogenerated chemiluminescence (ECL). The potentials generated in chronopotentiometry in a sample compartment are used to control the ECL in a separate detection compartment. A three-electrode cell is used to monitor the concentration changes of the analyte, while luminol-H_2O_2 system is responsible for ECL. The principle was shown to be feasible by theoretical simulations, indicating that the sampled times at a chosen potential, rather than traditional transition times, similarly give linear behavior between concentration and square root of sampled time. With the help of a voltage adapter, the experimental combination between chronopotentiometry and ECL was successfully implemented. As an initial proof of concept, the ferro/ferricyanide redox couple was investigated. The square root of time giving maximum light output changed linearly with ferrocyanide concentration in the range from 0.70 mM to 4.81 mM. The method was successfully applied to the visual detection of carbonate alkalinity from 0.06 mM to 0.62 mM using chronopotentiometry at an ionophore-based hydrogen ion-selective membrane electrode. The measurements of carbonate in real samples including river water and commercial mineral water were successfully demonstrated.

The signal conversion from electrochemical signals to visual readout is of great significance in analytical science, especially for the development of simple, easy to use and low-cost sensing devices. Electrochemical detection methods (voltammetry, amperometry, potentiometry, conductometry and electrochemical impedance spectroscopy) not only possess the advantages of simplicity, fast responses and ease of use, the instruments needed to perform the analysis can be miniaturized to low-cost microscale dimensions.[1-4] However, electrochemical signals are normally not intuitive and need numerical algorithms to allow for an interpretation of the data. Moreover, electrochemical methods become overly complex when extended to chemical detection in two dimensions and multiple channels. The visualization of chemical changes by means of imaging tools and parallel arrays has great promise for these applications.[5] It is therefore attractive to read out electrochemical signal with optical methods. Liu and Crooks previously developed a microelectrochemical sensing platform realizing such signal transduction through the electrochromic effect.[6] Gooding's group used similar electrochromic effect to read out potentiometric pH sensor and resistive-based sensors.[7,8] Wang and co-workers contributed a lot to the visualization of electrochemical sensing events based on bipolar electrodes.[9-14] Recently, our group reported on a strategy to convert potentiometric signals to a colorimetric readout through the turnover of a redox indicator in a thin layer using a closed bipolar electrode,[15] although this has not been applied to dynamic electrochemistry protocols such as chronopotentiometry. Electrochemical-to-optical signal transduction scheme was also demonstrated under chronoamperometry control with light-emitting diodes as indicators.[16]

In addition to color change, electrogenerated chemiluminescence (ECL) has also been used to provide a direct optical readout for potentiometric sensors.[17] ECL is an attractive combination of spectroscopic and electrochemical methodologies. It shows great potential for designing portable sensing devices because there is no need for an additional excitation light source and the ECL emission signal can be observed visually or with digital cameras.[18-24] In the above-mentioned work,[17] an ion-selective sensing electrode was placed in a sample physically separated from the ECL detection compartment. It was then treated as the reference electrode in order to modulate the potential at the working electrode used for ECL generation. Because two physically separate compartments were used for sensing and detection, ECL generation is not influenced by the sample composition.

Here, a general strategy is proposed to convert chronopotentiometric signals to ECL readout. In chronopotentiometry, a constant current is applied across the electrochemical cell. The output signal is the cell potential, which changes drastically at a so-called transition time. This transition time is concentration dependent and serves as the analytical signal. The strategy of this work is for the chronopotentiometric experiment to give a light pulse at a time that indicates the analyte concentration. This would be quite easily detectable by a camera or even by the naked eye and be a major advantage compared to intensity-based measurements for field deployable devices.

To achieve this, the time dependent potential change is applied to the detection compartment as voltage input to generate ECL. As luminol is one of the most efficient ECL luminophores, emitting blue liccght in the presence H_2O_2,[25-27] it was chosen to generate ECL. The concept is successfully demon-

strated with the ferro/ferricyanide redox couple at a conventional glassy carbon electrode and carbonate alkalinity detection at a hydrogen ion-selective electrode (ISE). Theoretical simulations accompany the experimental results. The use of the approach is demonstrated by visual detection of carbonate in river and commercial mineral water samples.

EXPERIMENTAL SECTION

Reagents. Potassium tetrakis[3,5-bis-(trifluoromethyl)phenyl]borate (KTFPB), tetrakis(4-chlorophenyl)borate tetradodecylammonium salt (ETH 500), chromoionophore I, 2-nitrophenyloctyl ether (o-NPOE), tris(hydroxymethyl)aminomethane (Tris), potassium ferricyanide, potassium ferrocyanide, acetic acid, sodium acetate, sodium chloride, luminol, hydrogen peroxide solution (35%), hydrochloric acid solution (1 M), and tetrahydrofuran (THF) were purchased from Sigma-Aldrich. All chemicals were of analytical grade and used without further purification.

Analytical Setup. A double-junction Ag/AgCl reference electrode was used in chronopotentiometric measurements (Mettler-Toledo AG, Schwerzenbach, Switzerland). Platinum electrode with a diameter of 3.0 mm (Metrohm, Switzerland) was used as counter electrode both in chronopotentiometric methods and ECL measurements. A glassy carbon electrode of 3.0 mm diameter purchased from Metrohm Autolab was used as working electrode to generate ECL and also used as working electrode in the ferrocyanide detection system. For ion-selective electrode preparation, electrode bodies (Oesch Sensor Technology, Sargans, Switzerland) were used to mount the ion-selective membranes. Porous polypropylene (PP) membranes (Celgard, 0.237 cm^2 surface area, 20 μm thickness) were kindly provided by Membrane Wuppertal, Germany. pH values were determined using a Metrohm 827 pH meter (Metrohm Autolab, Utrecht, The Netherlands).

The electrochemical measurements were performed with an Autolab PGSTAT128N (Metrohm Autolab, Utrecht, The Netherlands) controlled by a personal computer using Nova 2.1.3 software (supplied by Autolab). A panoramic picture of the setup is shown in Figure S1a. The homemade cell used for ECL measurement is shown in Figure S2b. ECL signals were video recorded by a digital camera (Canon EOS 5D Mark III with EF 100mm f / 2.8L Macro IS USM lens) operated in a dark box. The images of the ECL emission were extracted and analyzed by Wolfram Mathematica 11 software. A voltage adapter was designed and fabricated in house (picture shown in Figure S1c). It consists of an amplifier followed by an adder. The user can choose different fixed gains (0.5, 1, 2, 3, 5) and also set the offset (between -1V and +1V). The adapter circuit uses precision operational amplifiers (TI OPA277) that have low bias current and low offset voltage. They are powered internally using an internal DC/DC converter (XP Power IH0512S) that is followed by linear regulators (ST L7808 and ST L7809) that provides power rails at +8V and -8V. The gains are set using a rotary encoder that selects pre-calibrated feedback resistors that permits to choose the gain. While the offset is selected by a precision 10-turns potentiometer, its value is displayed on a display (TDE Instruments DPM961TG). A second display (TDE Instruments DPM961TG) is provided to read the output value.

Ion-selective Membrane Preparation. The ion-selective membrane for the detection of alkalinity was prepared according to the literature.[28] The cocktail H1 used for the membrane preparation was prepared by dissolving a mixture of 120 mmol/kg of hygrogen ionophore I, 60 mmol/kg of KTFPB, 90 mmol/kg of ETH 500 and 190 mg of o-NPOE in 1 mL of THF. The PP membrane used as supporting material was washed with THF for 10 min. When THF was completely evaporated, an excess volume of 4 μL of the cocktail H1 solution was deposited on the membrane. It was dried overnight at room temperature in a dust-free environment. After conditioning in buffer solution for 40 min, the membrane was mounted in the electrode body. The inner compartment was filled with 10 mM acetic acid/10 mM sodium acetate buffer (1/1) in 100 mM NaCl. All solutions were prepared in 100 mM NaCl as background electrolyte to minimize electrical migration.

Experimental Protocols. Chronopotentiometric experiments were performed in 100 mM NaCl as a background electrolyte with a galvanostatic pulse of 10 s. The potential was recorded as a function of time during the constant current pulse. After each chronopotentiometric determination, an opposite galvanostatic pulse was applied to recover the ferro/ferricyanide redox couple or to regenerate the ionophore-based hydrogen ion-selective membrane for carbonate detection.[29] For the ferrocyanide detection system, a constant current of 30 μA was applied and the dynamic response curves were obtained by adding predefined aliquots of standard solution (0.5 M potassium ferrocyanide solution and 0.5 M potassium ferricyanide solution) to a magnetically stirred background electrolyte. The use of equal amounts of ferricyanide and ferrocyanide maintains a stable starting potential of the system. For the carbonate sensing system, the stock solution was prepared from 1.0 M of carbonate and 1.0 M bicarbonate solution, adjusting the pH to 9.6. Calibration curves were obtained by adding precise amounts of carbonate stock solution into the magnetically stirred background electrolyte. Freely dissolved CO_2 was removed before measurements using nitrogen gas and a homemade capping seal.[29] Before each galvanostatic pulse, the pH value of the detection solution was measured with a Metrohm pH electrode and pH meter. The precise carbonate concentration was calculated from the pH value and the total carbonate concentration added. The potential generated in chronopotentiometry was output through the electrochemical workstation (Autolab PGSTAT128N) and modulated by the voltage adapter to fit the ECL requirements. The solution used in ECL emission was composed of 1 mM of luminol and 5 mM of H_2O_2 in 0.1 M of phosphate buffer solution (pH 11.0).

RESULTS AND DISCUSSION

Figure 1 shows the schematic configuration of the cell that achieves an ECL readout for a chronopotentiometric sensor. In chronopotentiometry, a constant current is applied across the electrochemical cell. The coutput signal is the cell potential, which changes over time and is applied to the detection compartment as voltage input to generate ECL. As time proceeds, the concentration of the electroactive species at the electrode surface will be depleted at a transition time τ, giving a drastic change in potential.[30-32] According to the Sand equation, the square root of the transition time should be linearly dependent on the concentration of the locally depleted species as follows:[33,34]

$$\frac{i\tau^{1/2}}{c_j} = \frac{nFAD_j{}^{1/2}\pi^{1/2}}{2} \quad (1)$$

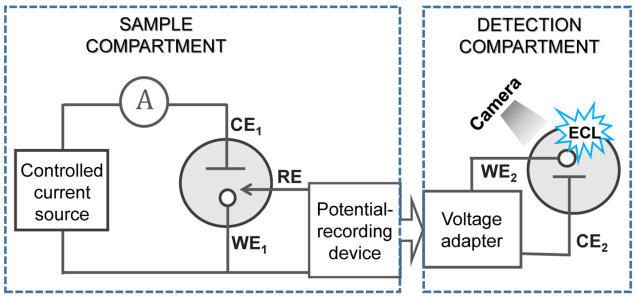

Figure 1. Schematic illustration of the proposed sensing approach converting chronopotentiometric signals in a sample compartment to a timed ECL pulse that can be captured by a camera. A glassy carbon electrode or an ion-selective electrode was used as the work-ing electrode (WE_1), platinum counter electrode (CE_1) and double-junction Ag/AgCl/3 M KCl/1 M LiOAc reference electrode (RE) were used in chronopotentiometric measurements. In ECL detection compartment, a glassy carbon electrode was used as the working electrode (WE_2) to generate light, and a platinum electrode was used as counter electrode (CE_2) to form a closed circuit.

where i is the applied current, c_j is the initial concentration of analyte j, n is the number of transferred electrons (for ion-selective membranes, n is instead z, the valency of j), F is the Faraday constant, A is the electrode area, and D_j is the diffusion coefficient of j. The time at which ECL reaches maximum intensity should coincide with chronopotentiometric transition time, which is achieved with the help of a voltage adapter. In this manner the analyte concentration in the samcple compartment may be translated into a time dependent light pulse.

To explain the working principle, a theoretical simulation of chronopotentiometric responses was made with the finite difference method (see the Supporting Information for details).[35] The simulated chronopotentiograms are shown in Figure 2a. The luminol/H_2O_2 system generates an ECL signal in the potential range from 0.2 V to 1.0 V and gives maximum intensity near 0.46 V on the surface of the glassy carbon electrode.[36-38] We therefore need to evaluate whether the square root of time at a given potential value (τ_E) still follows a linear relationship with analyte concentration. To test this, the times τ_E at which the chronopotentiometric responses reached a predefined potential for varying concentrations were extracted. Indeed, as shown in Figure 2b, the square root of τ_E shows a linear relationship with concentration. Surprisingly, linearity appears to hold even at chosen potentials that are far from the location of the inflection point.

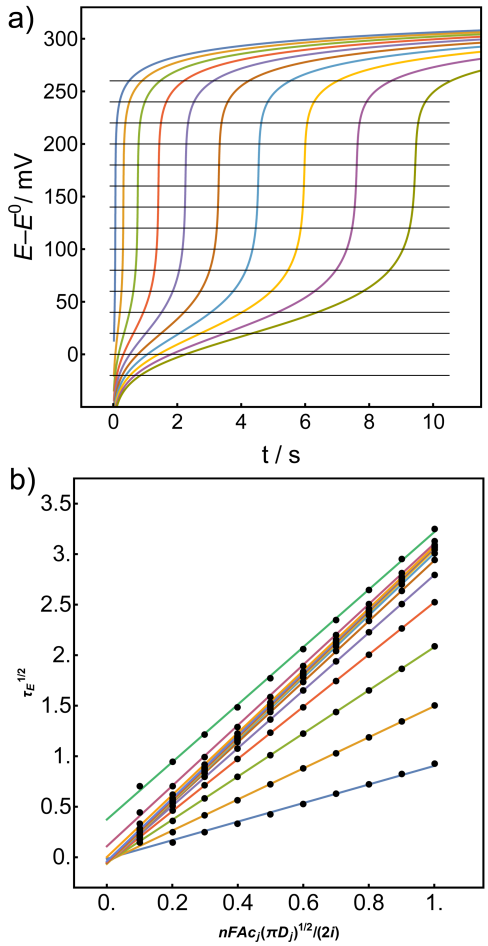

Figure 2. (a) Simulated chronopotentiograms for different analyte concentrations, see Supporting Information for details. (b) The points extracted at different fixed potential values in a) and the linear curves between the concentration and the square root of time for each potential (τ_E).

The linearity observed in Figure 2b suggests that if the ECL output describes a maximum at a predefined potential, the time at which maximum light intensity is recorded may now serve as analytical signal. To accomplish this, potential for ECL generation must be adapted to lie within the potential range of the chronopotentiometric response. This was accomplished with the help of a voltage adapter.

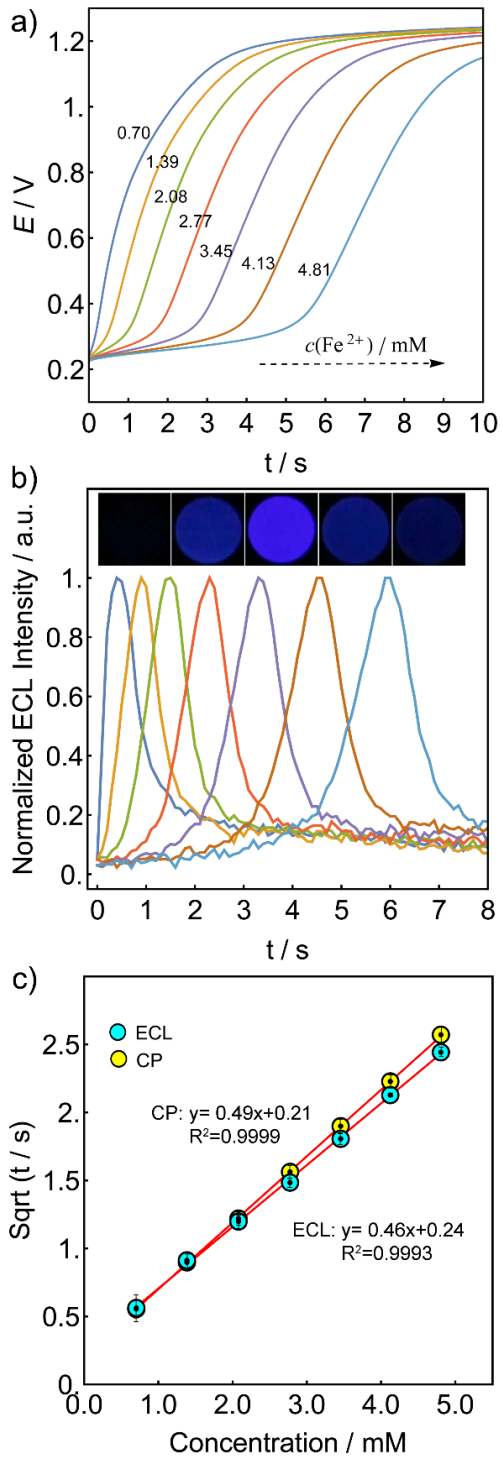

Figure 3. The combination of chronopotentiometry (CP) and ECL technique for the determination of ferrocyanide. (a) Potential changes during galvanostatic pulse of 30 µA for varying concentrations of ferrocyanide in 10 mM Tris-HCl buffer solution (pH 7.4) with 100 mM NaCl as background. (b) ECL responses for different concentrations. (Inset shows the change of ECL signals from dark to light and then back to dark.) (c) Linear calibration curves of the square root of the transition time in chronopotentiometry and of the time when ECL intensity reaches the maximum as function of concentration.

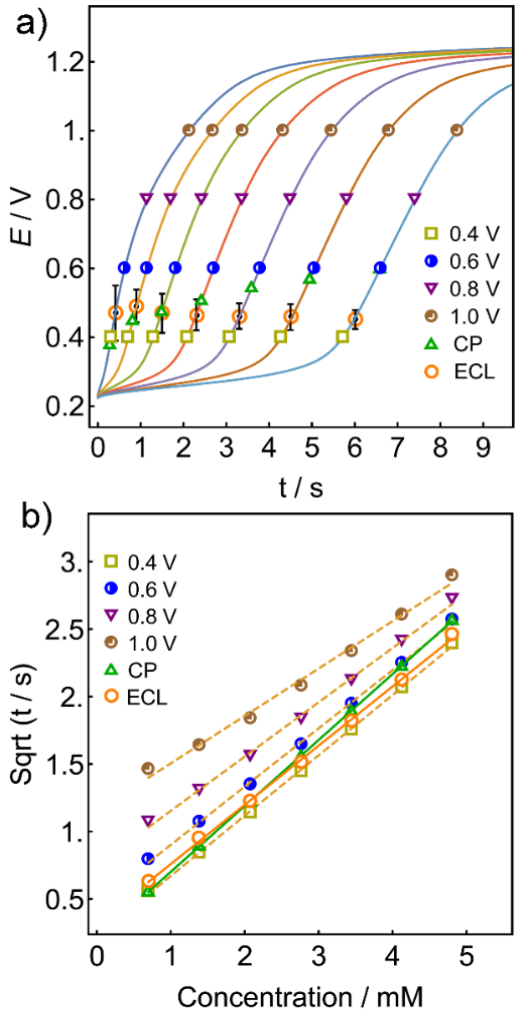

Figure 4. (a) The traditional transition time points (noted as CP), the corresponding times when ECL intensity reaches a maximum (noted as ECL) (error bars give potential range when ECL intensity varies from 95% to 100% of its peak) and the times at a predefined potential value as indicated. (b) Relationships between the ferrocyanide concentration and the square root of the transition time (noted as CP), the times at which ECL gives highest intensity (noted as ECL), and the times for the indicated predefined potential values.

As an initial proof of concept, the well-established ferri/ferrocyanide redox couple was investigated. The observed potential changes during a galvanostatic experiment for different concentrations of ferrocyanide are shown in Figure 3a. The concentration of ferrocyanide ions at the electrode surface changes with time, leading to a variation of potential. At the transition time, the depletion of ferrocyanide at the electrode surface occurs and a striking change in potential can be observed. The transition time can be easily observed by taking derivative of each chronopotentiogram, and a precise transition time can be extracted as the maximum of the time derivative of the potential (Figure S3).

A linear calibration curve between the square root of transition time and concentration is confirmed (Figure 3c). This three-electrode cell was now combined with the ECL detection compartment containing 1 mM of luminol and 5 mM of hydrogen peroxide. The corresponding ECL responses for different ferrocyanide concentrations are shown in Figure 3b (The video file in Supporting Information gives the ECL response at a 3.45 mM ferrocyanide concentration as example). The

luminol/H_2O_2 system tends to give a peak intensity near 0.46 V with a glassy carbon electrode,[36-38] while in the chronopotentiograms for the oxidation of ferrocyanide, the potential was found to change from 0.23 V to 1.23 V.

The maximum ECL signal happens to appear near the transition time point. Without additional potential offset, these two systems match well. As the concentration increases, it takes a longer time to observe the transition of the potential and a correspondingly longer time to record peak ECL output. As seen in Figure 3c, a linear relationship was established between the square root of t_p and the concentration of analyte, even though t_p is strictly not the same transition time as observed in chronopotentiometry. To clearly show the differences, every transition time point in chronopotentiometry and ECL peak time point is marked in the chronopotentiograms (Figure 4a). ECL peaks were observed around the potential of 0.47 V, while the transition time points in chronopotentiometry with increasing concentration vary as a function of the chosen fixed potential. The relationships between the concentration of analyte and the square root of time for given fixed potential values were then visualized in Figure 4b. Consistent with the theoretical predictions, they exhibit a good linearity in the potential range from 0.4 V to 0.8 V. Because most curves can be adequately described with the Sand equation, they should be adequate for analytical application to determine concentration. However, they should not be used for fundamental work, for example to extract diffusion coefficients and electrode surface area, because the slopes and intercepts deviate from that using traditional transition times. The deviation of the slope between traditional chronopotentiometric data and ECL readout can be mainly attributed to the increasing transition potentials in chronopotentiometry with increasing analyte concentration, see Figure 4b. While the two calibration curves are not strictly identical, they are both linear and should allow for a successful translation of transition time measurements to an ECL light pulse, as proposed here.

To demonstrate the versatility of this sensing approach, we applied it to the visual detection of carbonate alkalinity. Alkalinity is a critical parameter for evaluating water quality. Bicarbonate and carbonate are the predominant species that determine the alkalinity of environmental samples such as river wate and the determination of their concentration is of high significance. Here, WE_1 is an ion-selective membrane consisting of a polypropylene-supported liquid membrane doped with a hydrogen ionophore (chromoionophore I), ion exchanger (KTFPB), and lipophilic electrolyte (ETH 500). As introduced in previous work,[28] hydrogen ions expelled galvanostatically from the ion-selective membrane protonates available carbonate base in the diffusion layer via acid−base reaction. With time, the base species becomes depleted owing to the constant imposed hydrogen ion flux from the membrane, and a potential inflection occurs at a transition time τ, which is correlated to the concentration of the base in solution. As above, this potential change was converted to ECL emission signals, giving a light pulse readout for a direct carbonate alkalinity sensor. Figure 5a shows the chronopotentiograms for different concentrations of carbonate at a constant positive current of 20 μA. Transition times are then extracted from the time derivatives of the chronopotentiograms (Figure S4). However, the potential changes here from -0.1 V to 0.3 V, which is beyond the potential range for the ECL emission of the luminol/H_2O_2 system. For this reason, the potential input for ECL was adapted by using a voltage adapter. With this compact electronic device, the potential output from chronopotentiometry (U_1) may be adjusted as needed and used as input for ECL emission (U_2), performed with the formula:

$$U_2 = U_1 \times a + b \quad (2)$$

For carbonate detection, the optimum value of a and b was 2 and 0.15 V respectively, giving light output in the required potential range.

The normalized ECL intensity versus time profiles for different concentrations of carbonate are shown in Figure 5b. As the concentration of carbonate increases, the time used to observe the ECL peak intensity becomes longer. As above, the square root of this time exhibits a good linear relationship with carbonate concentration (Figure 5c). Similarly, a deviation also exists between the linear calibration curves of chronopotentiometric method and electrochemiluminescent results. A good linear relationships between the square root of time and concentration of the analyte were obtained at any chosen potential value in the range from 0.15 V to 0.25 V (Figure 6), which is again in agreement with theoretical expectations. This finding is welcome and confirms the practical applicability of the method. Yet, it not entirely expected because ECL intensity is known to not only depend on the applied potential but also on the rate of the potential change,[39,40] which tends to vary with concentration (Figure 5a).

The sensing mode was applied to the determination of carbonate in environmental samples from the Arve River in Geneva and commercial Evian mineral water. The total carbonate concentration (c_{tot}) in the samples is obtained from the carbonate concentration and the pH value of the detection solution (which is adjusted to about 9.6 in measurements). The carbonate species in the sample including carbonate (CO_3^{2-}), bicarbonate (HCO_3^-) and carbonic acid (H_2CO_3) can be calculated according to the following distribution equations (where δ represents the distribution fraction of carbonate speciation, and K_{a1} and K_{a2} are the dissociation constant of H_2CO_3 and HCO_3^-, respectively).

$$\delta_0 = \frac{[H_2CO_3]}{c_{tot}} = \frac{[H^+]^2}{[H^+]^2 + K_{a1}[H^+] + K_{a1}K_{a2}} \quad (3)$$

$$\delta_1 = \frac{[HCO_3^-]}{c_{tot}} = \frac{K_{a1}[H^+]}{[H^+]^2 + K_{a1}[H^+] + K_{a1}K_{a2}} \quad (4)$$

$$\delta_2 = \frac{[CO_3^{2-}]}{c_{tot}} = \frac{K_{a1}K_{a2}}{[H^+]^2 + K_{a1}[H^+] + K_{a1}K_{a2}} \quad (5)$$

The same sample was measured using an acidimetric titration as reference method, using phenolphthalein and bromocresol green as indicators. The results shown in Table 1 demonstrate that our visual detection method gives good quantitative agreement with the chronopotentiometric results and the standard titration method.

Table 1. Visual carbonate detection in real samples compared with different methods.

Sample	pH	[a]c_{tot}/mM	[b]$[CO_3^{2-}]$/mM	[b]$[HCO_3^-]$/mM	[b]$[H_2CO_3]$/mM	Method

Mineral water	7.21	6.69±0.10	0.00531±0.00008	5.82±0.09	0.861±0.013	ISE-ECL
		6.67±0.17	0.00530±0.00013	5.81±0.15	0.859±0.022	ISE-CP
		6.85±0.05	0.00544±0.00004	5.96±0.04	0.882±0.006	Titration
River water	8.28	2.88±0.10	0.0302±0.0010	2.81±0.10	0.0354±0.0012	ISE-ECL
		2.87±0.14	0.0301±0.0014	2.80±0.14	0.0353±0.0017	ISE-CP
		2.78±0.03	0.0291±0.0003	2.72±0.03	0.0342±0.0004	Titration

[a]Experimental values. [b]Calculated from the distribution equations. ISE-ECL means the ECL detection method combined with chronopotentiometry at the ion-selective electrode. ISE-CP means the chronopotentiometric method using ion-selective electrode.

CONCLUSIONS

We proposed here a general approach to read out chronopotentiometric sensors by a timed light pulse, using an ECL readout. For this purpose, the potential change over time in chronopotentiometric sensors was modulated to generate ECL in a separate detection compartment. The working principle of this method was first established with the help of theoretical simulations under the approximation that ECL peak signals appear at a constant potential. The feasibility of this strategy was then confirmed not only using conventional solid electrode for the determination of ferrous ions but also with ion-selective electrode for the detection of carbonate. Instead of ECL intensity, the time upon which ECL intensity reaches the maximum was measured to reflect the analyte concentration. It chiefly relies on the potential change for ECL generation, avoiding the influence from other interfering parameters on ECL intensity readouts, such as temperature, pH and concentration change of the detection solution. A timed light pulse is more easily detectable and quantifiable by mobile cameras than the traditional recording of intensities or potentials, which is attractive for field deployable devices as well as sensing arrays.

ASSOCIATED CONTENT

Supporting Information

The Supporting Information is available free of charge on the ACS Publications website.

Theory for the simulation of chronopotentiometric responses with the finite difference method, pictures of the experimental setup, time derivatives of the chronopotentiograms for the detection of ferrocyanide and carbonate (PDF).

An example of ECL response at 3.45 mM ferro/ferricyanide concentration (AVI).

AUTHOR INFORMATION

Corresponding Authors

* Xiaojiang Xie, E-mail: xiexj@sustc.edu.cn.
* Eric Bakker, E-mail: eric.bakker@unige.ch.

ACKNOWLEDGMENT

The authors thank the National Natural Science Foundation of China (21874063) and the Swiss National Science Foundation (200021_175622) for financial support.

REFERENCES

(1) Schwarz, M. A.; Hauser, P. C. *Lab Chip* **2001**, *1*, 1-6.
(2) Wang, J. *Talanta* **2002**, *56*, 223-231.
(3) Liana, D. D.; Raguse, B.; Gooding, J. J.; Chow, E. *Sensors* **2012**, *12*, 11505-11526.
(4) Freitas, M.; Nouws, H. P. A.; Delerue-Matos, C. *Electroanalysis* **2018**, *30*, 1576-1595.
(5) Chow, K.-F.; Mavré, F.; Crooks, J. A.; Chang, B.-Y.; Crooks, R. M. *J. Am. Chem. Soc.* **2009**, *131*, 8364-8365.
(6) Liu, H.; Crooks, R. M. *Anal. Chem.* **2012**, *84*, 2528-2532.
(7) Liana, D. D.; Raguse, B.; Gooding, J. J.; Chow, E. *ACS Appl. Mater. Inter.* **2015**, *7*, 19201-19209.
(8) Chow, E.; Liana, D. D.; Raguse, B.; Gooding, J. J. *Aust. J. Chem.* **2017**, *70*, 979-984.
(9) Zhang, X.; Chen, C.; Yin, J.; Han, Y.; Li, J.; Wang, E. *Anal. Chem.* **2015**, *87*, 4612-4616.
(10) Zhang, X.; Shang, C.; Gu, W.; Xia, Y.; Li, J.; Wang, E. *ChemElectroChem* **2016**, *3*, 383-386.
(11) Zhang, X.; Zhang, L.; Zhai, Q.; Gu, W.; Li, J.; Wang, E. *Anal. Chem.* **2016**, *88*, 2543-2547.
(12) Xing, H.; Zhang, X.; Zhai, Q.; Li, J.; Wang, E. *Anal. Chem.* **2017**, *89*, 3867-3872.
(13) Zhai, Q.; Fan, D.; Zhang, X.; Li, J.; Wang, E. *Npg Asia Mater.* **2017**, *9*, e421.
(14) Zhang, X.; Jing, Y.; Zhai, Q.; Yu, Y.; Xing, H.; Li, J.; Wang, E. *Anal. Chem.* **2018**, *90*, 11780-11784.
(15) Jansod, S.; Cuartero, M.; Cherubini, T.; Bakker, E. *Anal. Chem.* **2018**, *90*, 6376-6379.
(16) Zhai, J.; Yang, L.; Du, X.; Xie, X. *Anal. Chem.* **2018**, *90*, 12791-12795.
(17) Crespo, G. A.; Mistlberger, G.; Bakker, E. *J. Am. Chem. Soc.* **2012**, *134*, 205-207.
(18) Knight, A. W. *TrAC-Trend. Anal. Chem.* **1999**, *18*, 47-62.
(19) Fahnrich, K. A.; Pravda, M.; Guilbault, G. G. *Talanta* **2001**, *54*, 531-559.
(20) Richter, M. M. *Chem. Rev.* **2004**, *104*, 3003-3036.
(21) Marquette, C. A.; Blum, L. J. *Anal. Bioanal. Chem.* **2008**, *390*, 155-168.
(22) Miao, W. *Chem. Rev.* **2008**, *108*, 2506-2553.
(23) Liu, Z.; Qi, W.; Xu, G. *Chem. Soc. Rev.* **2015**, *44*, 3117-3142.
(24) Gao, W.; Saqib, M.; Qi, L.; Zhang, W.; Xu, G. *Curr. Opin. Electrochem.* **2017**, *3*, 4-10.
(25) Fähnrich, K. A.; Pravda, M.; Guilbault, G. G. *Talanta* **2001**, *54*, 531-559.
(26) Gao, W.; Muzyka, K.; Ma, X.; Lou, B.; Xu, G. *Chem. Sci.* **2018**, *9*, 3911-3916.
(27) Hu, L.; Xu, G. *Chem. Soc. Rev.* **2010**, *39*, 3275-3304.
(28) Afshar, M. G.; Crespo, G. A.; Xie, X.; Bakker, E. *Anal. Chem.* **2014**, *86*, 6461-6470.
(29) Jarolimova, Z.; Crespo, G. A.; Xie, X.; Afshar, M. G.; Pawlak, M.; Bakker, E. *Anal. Chem.* **2014**, *86*, 6307-6314.
(30) Bard, A. J.; Faulkner, L. R. *Wiley: New York* **2001**, *7*, 255.
(31) Gemene, K. L.; Bakker, E. *Anal. Chem.* **2008**, *80*, 3743-3750.
(32) Jarolimova, Z.; Crespo, G. A.; Afshar, M. G.; Pawlak, M.; Bakker, E. *J. Electroanal. Chem.* **2013**, *709*, 118-125.
(33) Sand, H. J. S. *Phil. Mag.* **1901**, *1*, 45-79.
(34) Bard, A. J. *Anal. Chem.* **1961**, *33*, 11-15.
(35) Yuan, D.; Cuartero, M.; Crespo, G. A.; Bakker, E. *Anal. Chem.* **2017**, *89*, 586-594.
(36) Liu, X.; Qi, W.; Gao, W.; Liu, Z.; Zhang, W.; Gao, Y.; Xu, G. *Chem. Commun.* **2014**, *50*, 14662-14665.
(37) Sakura, S. *Anal. Chim. Acta* **1992**, *262*, 49-57.

(38) Vitt, J. E.; Johnson, D. C.; Engstrom, R. C. *J. ElectroChem. Soc.* **1991**, *138*, 1637-1643.
(39) Choi, J.-P.; Bard, A. J. *Anal. Chim. Acta* **2005**, *541*, 141-148.
(40) Cui, H.; Zhang, Z. F.; Zou, G. Z.; Lin, X. Q. *J. Electroanal. Chem.* **2004**, *566*, 305-313.

TOC

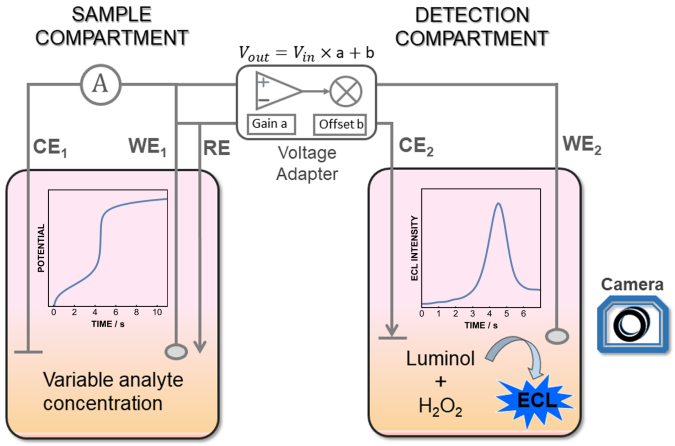
SAMPLE
COMPARTMENT
DETECTION
COMPARTMENT
$V_{out} = V_{in} \times a + b$
A
Gain a
Offset b
Voltage
Adapter
CE1
WE1
RE
CE2
WE2
POTENTIAL
TIME / s
ECL INTENSITY
TIME / s
Camera
Variable analyte
concentration
Luminol
+
H_2O_2
ECL

Supporting Information For:

Electrogenerated Chemiluminescence for Chronopotentiometric Sensors

Wenyue Gao,[†,‡] Stéphane Jeanneret,[†] Dajing Yuan,[†] Thomas Cherubini,[†] Lu Wang,[†] Xiaojiang Xie[‡,*] and Eric Bakker[†,*]

[†] Department of Inorganic and Analytical Chemistry, University of Geneva, Quai Ernest-Ansermet 30, CH-1211 Geneva, Switzerland

[‡] Department of Chemistry, Southern University of Science and Technology, Shenzhen, 518055, China

* E-mail: xiexj@sustc.edu.cn; eric.bakker@unige.ch.

Table of Contents:

Theory:

In chronopotentiometric sensors, a galvanostatic pulse applied to the electrochemical cell induces a diffusion flux of a redox active species j from the sample solution to the electrode surface:[1]

$$i = n_j F A J_j \tag{S1}$$

where i is the applied current and A is the electrode surface area. Assuming that the electrochemical reaction is sufficiently fast and one-dimensional diffusion is the predominant form of mass transport, the ion flux J_j at the sample-electrode interface ($x = 0$) can be described as follows (D_j corresponds to the diffusion coefficient of species j):

$$J_j = -D_j \left[\frac{\partial c_j(x,t)}{\partial x}\right]_{x=0} \tag{S2}$$

Time dependent phenomena are simulated by the finite difference method.[2] For this purpose, we use the continuity equation as:

$$\frac{\partial c_j(x)}{\partial t} = \frac{\partial J_j(x)}{\partial x} \tag{S3}$$

In a numerical simulation with equal distance steps (d), we assume linear gradients from any step v to step $(v+1)$.[1] Eqn. S2 is rewritten as

$$J_{j,v/v+1}(t) = -D_j \frac{c_j(v+1,t) - c_j(v,t)}{d} \tag{S4}$$

where $J_{j,v/v+1}(t)$ is the flux from v th to the $(v+1)$ th element and $c_j(v,t)$ is the concentration in the respective element. The continuity in Eqn. S3 is rewritten as:

$$\frac{c_j(v,t+\Delta t) - c_j(v,t)}{\Delta t} = \frac{J_{j,v-1/v}(t) - J_{j,v/v+1}(t)}{d} \tag{S5}$$

Inserting Eqn. S4 into Eqn. S5 for the indicated position gives:

$$\frac{c_j(v,t+\Delta t) - c_j(v,t)}{\Delta t} = D_j \frac{c_j(v-1,t) - c_j(v,t)}{d^2} - D_j \frac{c_j(v,t) - c_j(v+1,t)}{d^2} \tag{S6}$$

which is solved for each position v for the concentration of the following step:

$$c_j(v,t+\Delta t) = c_j(v,t) + \frac{\Delta t}{d^2} D_j \left[c_j(v-1,t) - 2c_j(v,t) + c_j(v+1,t)\right] \tag{S7}$$

If one takes the first element near the electrode surface as the position 0, one can relate the applied current to the diffusional flux on the basis of the Fick's first law as follows:

$$i = n_j F A J_j(\mathrm{t}) = -n_j F A D_j \frac{(c_j(1,t) - c_j(0,t))}{d} \tag{S8}$$

Once one has defined initial conditions for the experiments in all elements of distance d, the applied current amplitude is used to calculate the concentration change at position 0 near the electrode surface, while all other concentrations for the next time step can be derived from Eqn. S7. The associated potential change based on the Nernst equation was simulated from the concentrations at the position of 0.

Consider two redox active species are present in solution, here labeled as O and P (whose initial total concentration is labeled as c_O^{tot} and c_P^{tot}, respectively). Before the transition time, the applied current was carried by species O. The Nernst equation can be written as:

$$E = E_O^{0\prime} - \frac{s}{n_o}\log\frac{c_O}{c_O^{tot} - c_O} \quad \text{(S9)}$$

Eqn. S8 can be rewritten as:

$$i = n_O F A J_O(\mathrm{t}) = -n_O \mathrm{F} A D_O \frac{\left(c_O(1,t) - c_O(0,t)\right)}{d} \quad \text{(S10)}$$

As time proceeds, the surface concentration will deplete to zero at a transition time τ, and a sudden potential change is observed. After this transition time, a different redox couple P will become dominant to maintain the ion flux. The Nernst equation can be written as:

$$E = E_P^{0\prime} - \frac{s}{n_P}\log\frac{c_P}{c_P^{tot} - c_P} \quad \text{(S11)}$$

Similarly, Eqn. S8 for species P can be rewritten as:

$$i = n_P F A J_P(\mathrm{t}) = -n_P \mathrm{F} A D_P \frac{\left(c_P(1,t) - c_P(0,t)\right)}{d} \quad \text{(S12)}$$

The expected chronopotentiogram is calculated from the concentration and using the Nernst equation, considering that the background species P does not deplete during the experiment.

Parameters used for simulation:

n_O = 1, n_P = 1, i = 6 μA, A = 7.0 mm^2, F = 96485 C/mol, D_j = 1×10^{-5} cm^2/s, d = 5×10^{-5} dm, Δt = 0.01 s, c_P^{tot} = 0.1 M, c_O^{tot} ranges from 0.1 mM to 1.0 mM.

References:

(1) Gemene, K. L.; Bakker, E. *Anal. Chem.* **2008**, *80*, 3743-3750.

(2) Yuan, D.; Cuartero, M.; Crespo, G. A.; Bakker, E. *Anal. Chem.* **2017**, *89*, 586-594.

Figures：

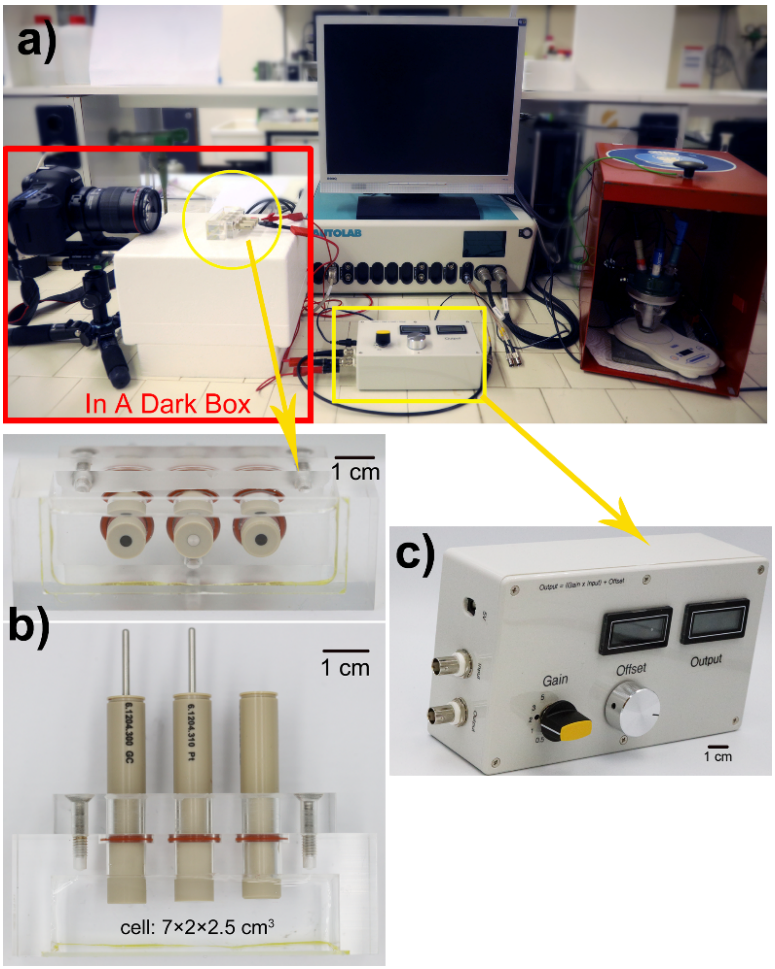

Figure S1. Pictures of the experimental setup. (a) A panoramic picture of the setup. (b) Pictures of the homemade cell for ECL measurements. Two electrodes were used including glassy carbon working electrode and platinum counter electrode. (c) The voltage adapter used to modulate the potential for ECL.

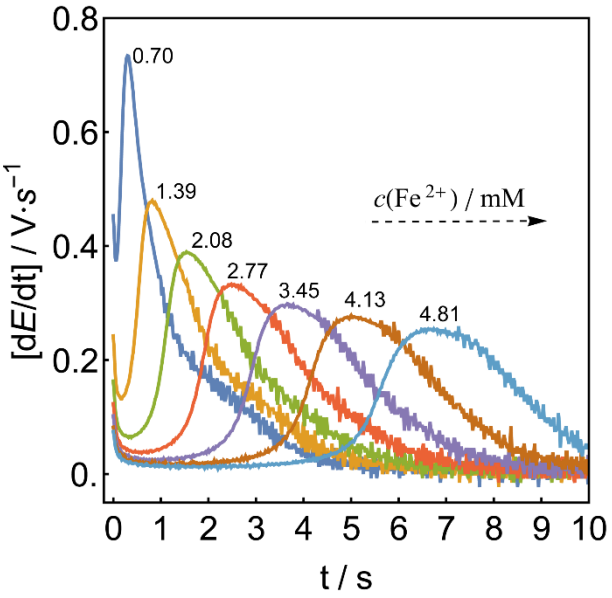

Figure S2. Time derivatives of the chronopotentiograms for varying concentrations of ferrocyanide in 10 mM Tris-HCl buffer solution (pH 7.4) with 100 mM NaCl as background.

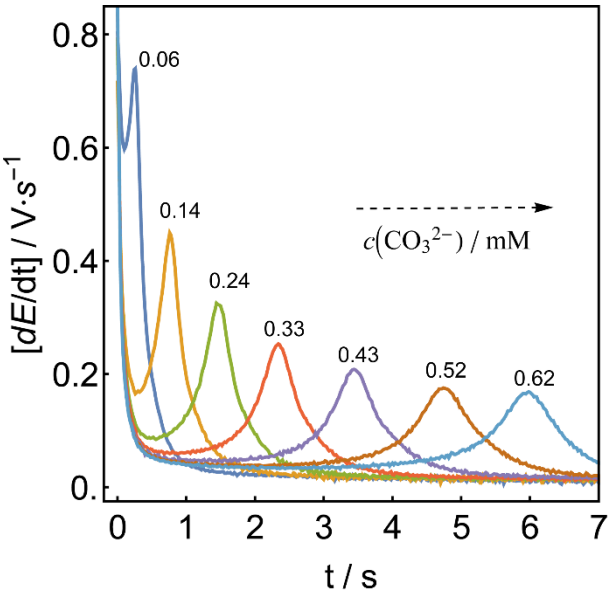

Figure S3. Time derivatives of the chronopotentiograms for increasing concentrations of carbonate.